

GRZEGORZ BOSAK*

WIND TUNNEL TESTS OF THE EFFECTS OF AERODYNAMIC INTERFERENCE ON A STADIUM ROOF

BADANIA MODELOWE WPŁYWÓW INTERFERENCJI AERODYNAMICZNEJ NA ZADASZENIE STADIONU

Abstract

This paper summarizes results of wind tunnel tests of a non-standard stadium roof. Aerodynamic laboratory studies were accomplished in a boundary layer wind tunnel. The main objective of the research was to determine the distribution of the mean wind net pressure coefficient over the stadium roof surfaces as affected by the aerodynamic interference between the stadium structure and a large oval sports event hall, located nearby. Interference coefficients of wind pressure and global wind forces acting upon the surfaces of the stadium roof were calculated. The aerodynamic studies showed a significant influence of the oval Atlas Arena sports-event hall on the wind load subjected to the stadium structure.

Keywords: wind tunnel tests, aerodynamic interference, wind action on a stadium roof

Streszczenie

W artykule przedstawiono rezultaty badań modelowych w tunelu aerodynamicznym niestandardowego zadaszenia stadionu. Badania zostały wykonane w tunelu aerodynamicznym z warstwą przyścienną. Podstawowym celem analiz było określenie rozkładu wartości współczynnika średniego ciśnienia wiatru na powierzchniach zadaszenia w warunkach występowania interferencji aerodynamicznej pomiędzy konstrukcją stadionu a rozległą owalną halą widowiskowo-sportową położoną w bliskim sąsiedztwie. Wyznaczono współczynniki interferencji odnoszące się do ciśnienia wiatru na powierzchni zadaszenia oraz do sumarycznych sił działania wiatru na konstrukcję dachu stadionu. Badania wykazały znaczący wpływ hali widowiskowo-sportowej Atlas Areny na działanie wiatru na konstrukcję stadionu.

Słowa kluczowe: badania modelowe w tunelu aerodynamicznym, interferencja aerodynamiczna, działanie wiatru na zadaszenie stadionu

* Ph.D. Grzegorz Bosak, Department of Structural Mechanics, Faculty of Civil Engineering, Cracow University of Technology, Cracow, Poland.

1. Introduction

The subject of the article is to evaluate the influence of aerodynamic interference on the wind action on a stadium roof. There were three circumstances which gave reasons for an aerodynamic modelling of the stadium roof structure in a wind tunnel. Firstly, the stadium roof was open to the north-west (see Fig. 1a)). What is more, in the geographical region of concern, this coincides with the direction of the most frequent strong winds. Secondly, a large oval sports event hall was located nearby (see Fig. 1b)). This could result in a significant aerodynamic interference affecting the stadium roof. Finally, the shape of the roof membrane was similar to a funnel (see Fig. 1c)), which could cause complex and various wind pressure distributions on the roof surfaces and as a result, difficulties in predicting wind action on the main bearing steel frames (see Fig. 1d)) during the design stage.

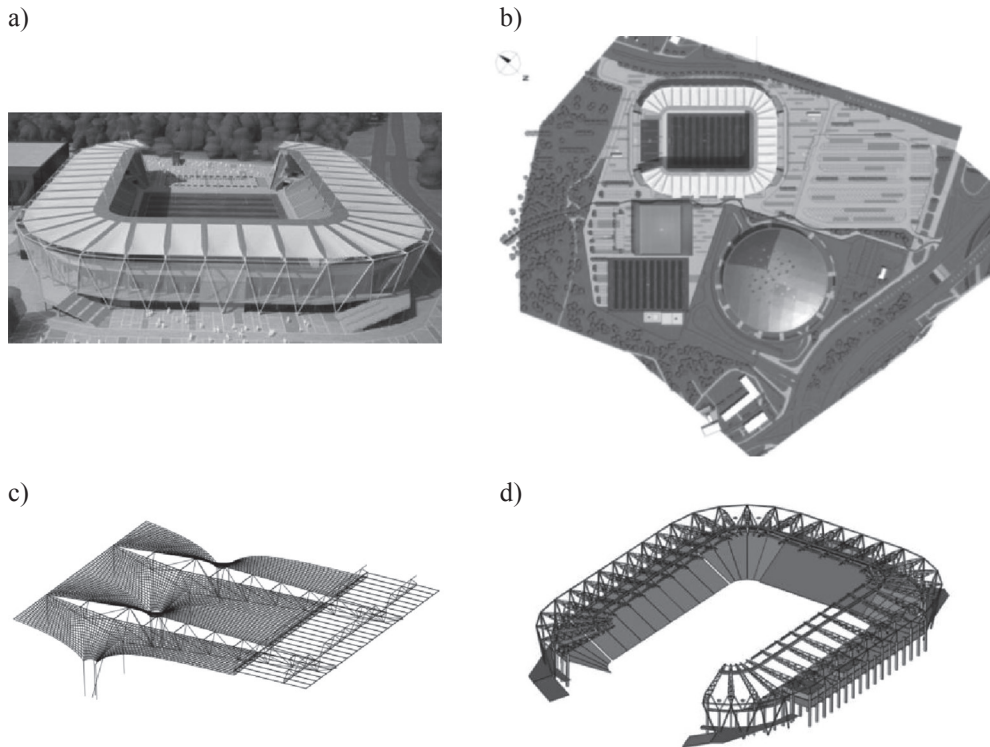


Fig. 1. Computer visualization: a) of the stadium structure, b) of the stadium with the immediate surroundings, c) of the shape of the stadium roof membrane; d) of the main bearing system of the stadium roof

The roof surface consists of a funnel shaped region and a flat inner ring (see Fig. 1c)). The structure is not symmetrical from an aerodynamic point of view. The stadium stands and stadium building objects have different configurations in particular parts of the structure (see Fig. 1d) and Fig. 2).

As can be seen in Fig. 1a), the whole roof surface is divided into 39 segments. Each segment is placed between the main steel frames and has a complex geometrical shape (see Fig. 1c)). In addition, the stadium façade is made of claddings which are permeable to air.



Fig. 2. Computer visualization of the stadium facades

All the above mentioned reasons motivated an aerodynamic wind tunnel investigation of a model.

2. Characteristics of the wind tunnel tests

The wind tunnel tests were conducted, using 1:200 scale stadium model, in the wind tunnel of the Wind Engineering Laboratory of Cracow University of Technology. The stadium and its immediately surrounding area within a radius of 250 m was modelled. This mainly consists of two structures: the stadium structure and the oval sports-event hall. Additionally, a training hall located near the stadium was taken into consideration. During the wind tunnel tests of the aerodynamic interference, the stadium and the training hall were studied as one object (see Fig. 3a)).

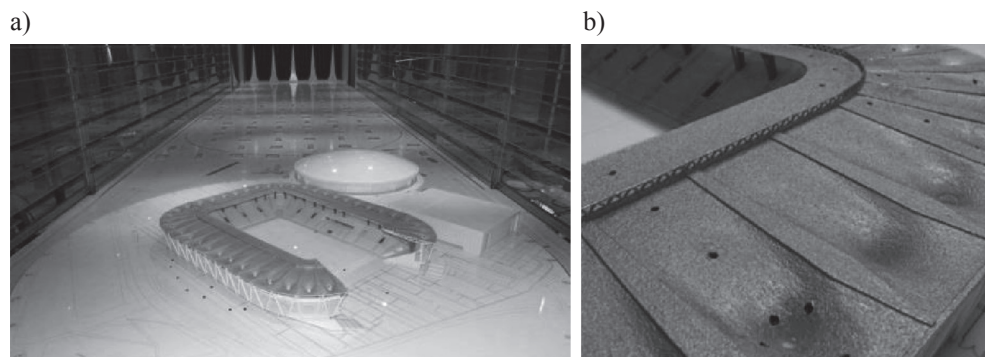


Fig. 3. a) stadium model with its immediate surroundings in the wind tunnel working section,
b) a part of the stadium roof model with pressure taps

The stadium model, at a scale of 1:200, and the other model objects of the immediate surroundings were placed on a 200 cm diameter turn-table, which allowed for the simulation of any wind direction in the working section. The measurements were taken for 36 wind directions with steps of 10° each. The model was instrumented with 224 pressure taps (see Fig. 3b)). The mean wind pressure and the standard deviation of wind pressure fluctuations were measured at each tap. On the basis of the measured data, mean pressure coefficients were calculated. A view of the tested model in the wind tunnel working section is presented in Fig. 3a).

The experiments were performed for the following conditions: power law exponent of mean wind velocity profile $\alpha = 0.3$; area-averaged turbulence intensity on the level of the stadium roof $I_v = 20\%$; reference velocity on the height level of the stadium roof model $V_{ref} = 13.5$ m/s. All of the wind tunnel properties such as the configuration of an adjustable ceiling, ejection of floor blocks, RPM of the fan, type of circulation, settings of barrier and spires had been optimised due to the model size, its scale, external shape, and roughness of the terrain. The mean wind velocity profile obtained in the wind tunnel working section during the experiments is presented in Fig. 4.

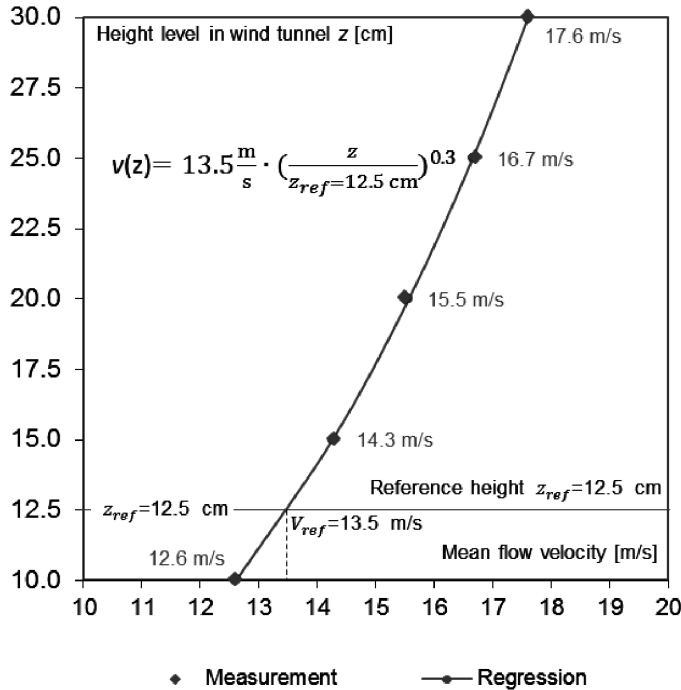


Fig. 4. Mean wind velocity profile obtained in the wind tunnel working section

A profile pressure probe, a pressure electronic scanner, which allow measuring differential pressure (a difference between the wind pressure on the top surface and the wind pressure on the bottom surface of the stadium roof membrane) in 64 taps simultaneously, and a hot-wire anemometer system were used during the experiments. The tunnel investigations were based on methodology presented in [1].

Below, in Fig. 5, a flow chart of the measuring system of differential wind pressure on the roof surfaces is presented.

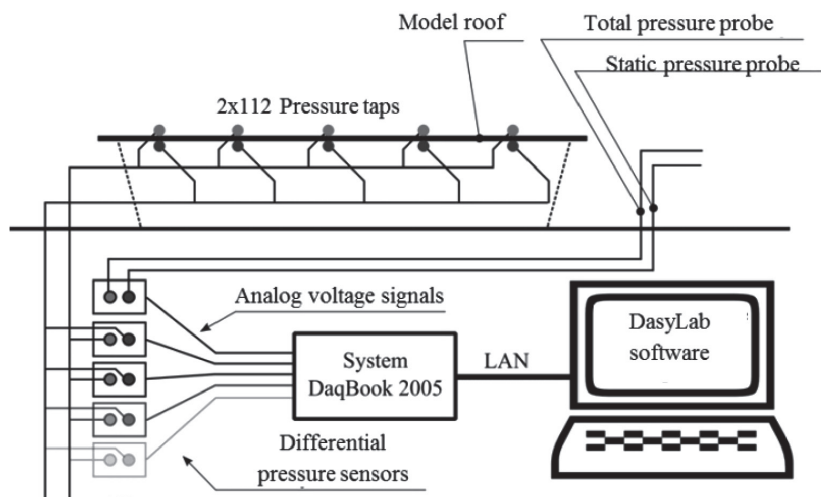


Fig. 5. The flow chart of the measuring system of differential wind pressure on the roof surface

Two measuring configurations, a non-interference configuration and an interference configuration, were considered during the experiments (see Fig. 6). In the first configuration, the measurements were conducted without any influence from the stadium neighbourhood. Subsequently, in the second configuration, the existence of the surrounding sports-event hall was taken into consideration during the tunnel test. Additionally, wind directions analysed during the experiments are presented in Fig. 6.

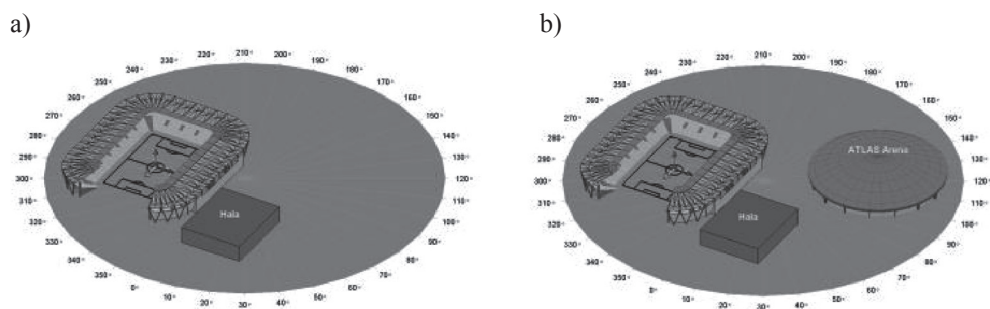


Fig. 6. Measuring configurations: a) a non-interference configuration, b) an interference configuration

The comparison of the results, namely the values of the wind pressure coefficients and the components of the global wind forces acting on each of the 39 roof segments, was accomplished on the basis of the test results for the two analysed configurations.

3. Results of the wind tunnel tests

The results of the values of the $C_{p,net}$ coefficient were determined in the non-interference and the interference configurations according to the formula (1):

$$C_{p,net}(x, y, z, dir) = \frac{\bar{p}_{net}(x, y, z, dir)}{q_{ref}(z_{ref})} \quad (1)$$

The reference level z_{ref} was at a height of the top level of the stadium model roof (equivalent to 25 m above ground in full scale). Negative values of wind pressure lift the roof membrane up. Below, in Fig. 7, exemplary distributions of $C_{p,net}$ coefficient in the interference configuration for the chosen wind directions are presented.

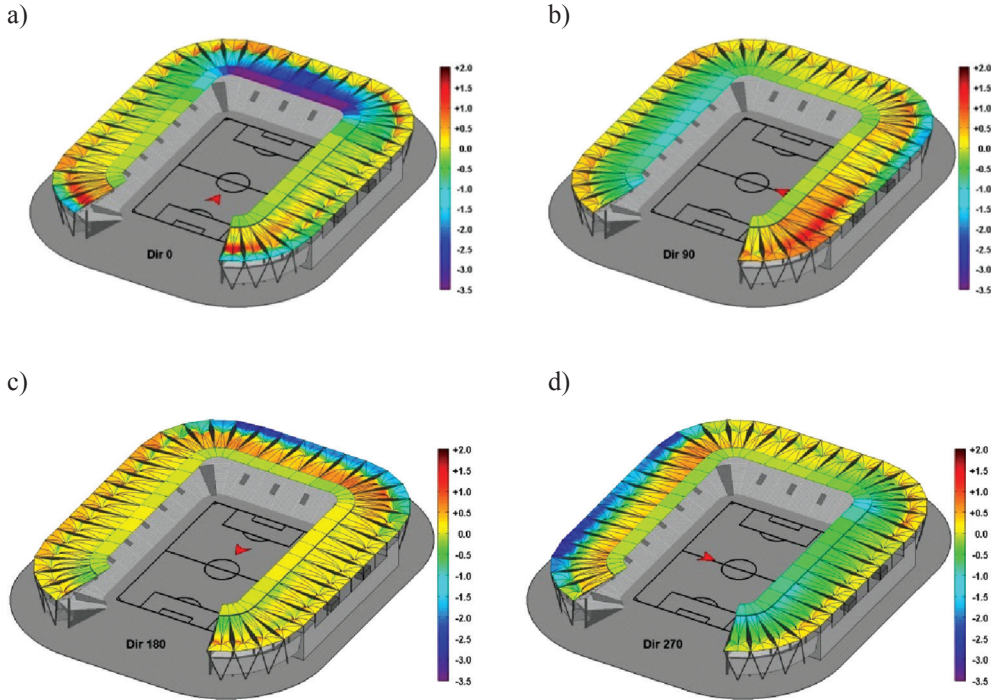


Fig. 7. Distributions of $C_{p,net}$ coefficient in the interference configuration for the chosen wind directions (a red arrow indicates the wind direction)

The values of the wind differential pressure coefficients are between +2.0 (positive pressure) and -3.5 (negative pressure). It is observed that the open geometry of the stadium roof caused an unfavourable aerodynamic effect, which consists of the occurrence of a huge uplift wind load for the fragment of the roof located in the opposite side to the open region of the stadium. This effect is strongly observed for the wind directions described by the angle values near 0°. In this roof region, the wind differential pressure coefficient reached the value

of -3.5 (see Fig. 7a)). The funnel shape of the stadium roof membrane caused significant variation of wind pressure distribution on the analysed surfaces. The positive differential wind pressure was applied over the leeward membrane area placed behind the funnel, which pressed this roof region down. This was as a result of the funnel wake existence at the below side of the stadium membrane. The windward region was lifted where the considerable negative net wind pressure occurred. This is observed very clearly in Fig. 7d).

In full scale, the global aerodynamic forces for the inner ring and the funnel area of the stadium roof were separately calculated by using distributions of the $C_{p,net}$ coefficient obtained from the measurements according to the formula (2):

$$F_k(dir, seg, area) = q_{ref}^p(z_{ref}) \sum_{A_{seg,area}} C_{p,net}(x, y, z, dir) \cdot \Delta A_{seg,area}(x, y, z) \cdot n_k(x, y, z) \quad (2)$$

where:

- dir – wind direction,
- k – coordinates x, y, z ,
- seg – the segment region (total number of segments was equal to 39),
- $area$ – the inner ring area or the funnel area,
- ΔA – a part of the area of the roof surface,
- n_k – a coordinate of the unit vector, perpendicular to the roof surface.

Coordinate systems of the global aerodynamic forces for the inner ring and the funnel area of the stadium roof are presented in Fig. 8.

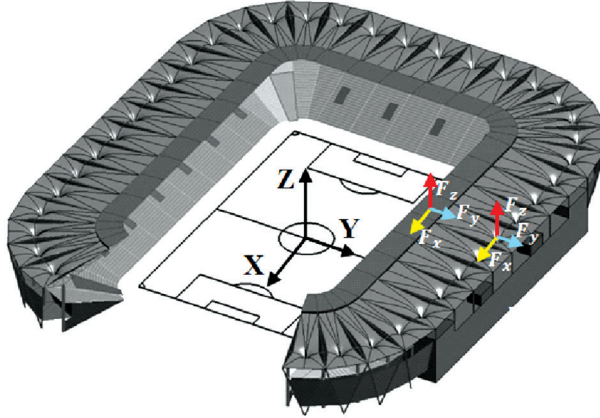
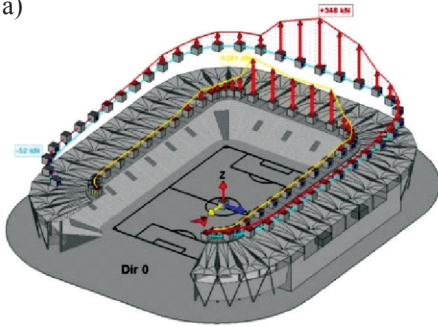


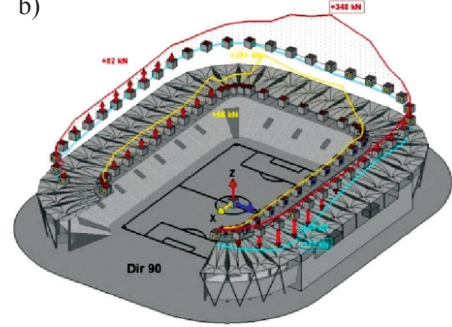
Fig. 8. Coordinate systems of the global aerodynamic forces for the inner ring and the funnel area of the stadium roof

The chosen distributions of the global aerodynamic forces for the inner ring and the funnel area, in relation to the force envelopes in the interference configuration, are presented in Fig. 9.

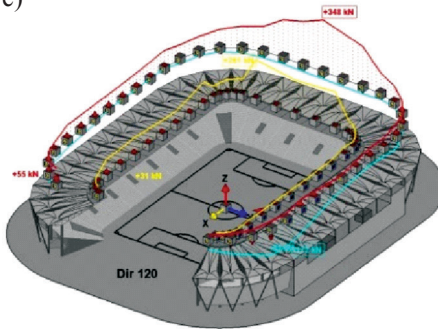
a)



b)



c)



d)

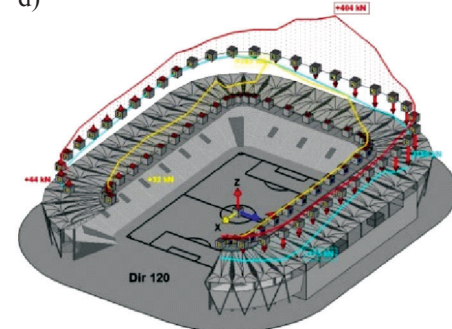
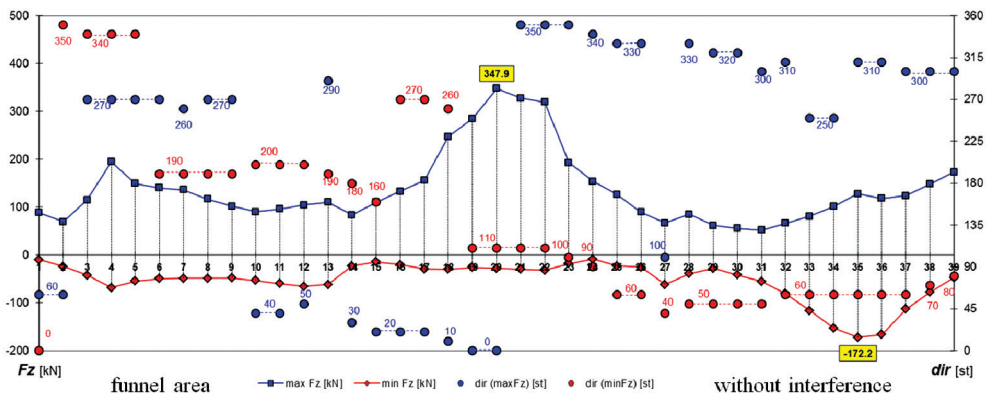


Fig. 9. Distributions of the global aerodynamic forces for the inner ring and the funnel area in relation to the force envelopes in the interference configuration

In Figs. 10 and 11, the envelopes of the global aerodynamic forces for the funnel area and the inner ring in the non-interference and interference configurations are presented. Wind directions, referring to the values of the wind force envelopes for any of 39 segments of the stadium roof, were introduced in the figures presented below.



A importance of the aerodynamic interference for the changing of the wind pressure on the roof surface was determined by the interference coefficient I_c^p [2] obtained according to formula (3):







$$I_c^p(x, y, z, dir, type, area) = \frac{\left| \left[C_{p,net}^I(x, y, z, dir) - C_{p,net}^S(x, y, z, dir) \right]_{type} \right|}{\max \left| C_{p,net}^S(x, y, z, dir) \right|_{area}} \quad (3)$$

where:

- dir – wind direction,
- x, y, z – point coordinates,
- I – interference configuration,
- S – non-interference configuration,
- $type$ – the type of wind pressure variation on the roof surfaces according to Tab. 1,
- $area$ – the inner ring area or the funnel area.

Table 1

Types of wind pressure coefficients changing on the roof surface

Type	Change type	Colour mark	$C_p^I(x, y, z, dir)$	$C_p^S(x, y, z, dir)$	$C_p^I(x, y, z, dir) - C_p^S(x, y, z, dir)$
6	$pos \uparrow$		$C_p^I > 0$	$C_p^S \geq 0$	$C_p^I - C_p^S > 0$
5	$pos \downarrow$		$C_p^I \geq 0$	$C_p^S \geq 0$	$C_p^I - C_p^S \leq 0$
4	$neg \uparrow pos$		$C_p^I \geq 0$	$C_p^S < 0$	$C_p^I - C_p^S > 0$
3	$pos \downarrow neg$		$C_p^I \leq 0$	$C_p^S > 0$	$C_p^I - C_p^S < 0$
2	$neg \uparrow$		$C_p^I \leq 0$	$C_p^S < 0$	$C_p^I - C_p^S \geq 0$
1	$neg \downarrow$		$C_p^I < 0$	$C_p^S \leq 0$	$C_p^I - C_p^S < 0$

The most significant influence of the aerodynamic interference between the stadium and the oval sports-event hall was observed for the wind direction of 120° . This situation is presented in Fig. 12, where the stadium structure was sheltered by the oval sports event hall (to be located on the leeward side of the oval sports-event hall – see Fig. 6b)).

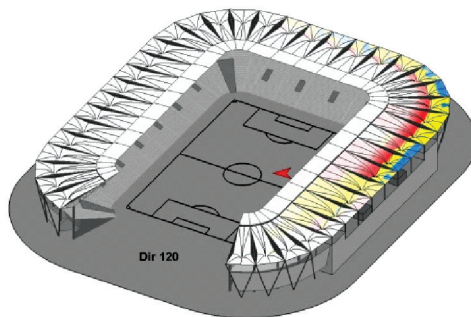
The maximum values of the pressure interference coefficient with division into six types of wind pressure change are presented in Tab. 2. According to the wind tunnel tests, the largest influence of the aerodynamic interference, connected with the existence of the neighbouring sports event hall, was observed for a limited area of stadium roof situated near the neighbouring structure. Mostly, the effect of aerodynamic interference consisted of pressing the roof membrane down (see the area of wind pressure change of types 2, 4, 6 in Fig. 12). No noticeable influence was observed for the inner ring area of the roof.

To compare the global vertical aerodynamic force component acting on each of 39 roof segments, an interference coefficient $I_c^{F_z}$ was calculated using the formula (4):

Table 2

Maximum values of I_c^p

Type	Funnel area	Inner ring area
6	0.92	0.03
5	0.23	0.01
4	0.98	0.03
3	0.30	0.01
2	0.93	0.26
1	0.51	0.31

Fig. 12. Distribution of I_c^p coefficient for 120° wind direction in the interference configuration

$$I_c^{F_z} (dir, area) = \frac{|F_z^I (dir, area)| - |F_z^S (dir, area)|}{\max |F_z^S (dir)|_{area}} \cdot 100\% \quad (4)$$

where:

- F_z – vertical component of the aerodynamic force acting on the particular segment of the inner area or the funnel area,
- dir – wind direction,
- I – interference configuration,
- S – non-interference configuration,
- $area$ – the inner ring area, the funnel area.

The distributions of I_c^F coefficient values are presented in Fig. 13. The largest influence of the aerodynamic interference was observed for the funnel area of 27th segment (see Tab. 3). In this case, the wind direction angle was equal to 120°. The stadium roof regions of the significant aerodynamic interference effects were placed over the funnel area located near the sports event hall. The interference influence from the neighbouring structure consisted largely in pressing the stadium roof down in cases where the roof funnel area of the stadium was placed into the aerodynamic wake of the sports-event hall.

Table 3

Extreme values of I_c^F coefficient

Area	Funnel region		Inner ring region	
Extreme	Max	Min	Max	Min
Value of I_c^F [%]	+190%	−56%	+31%	−26%
Segment	27	29	7	31
Wind direction	120°	90°	30°	290°

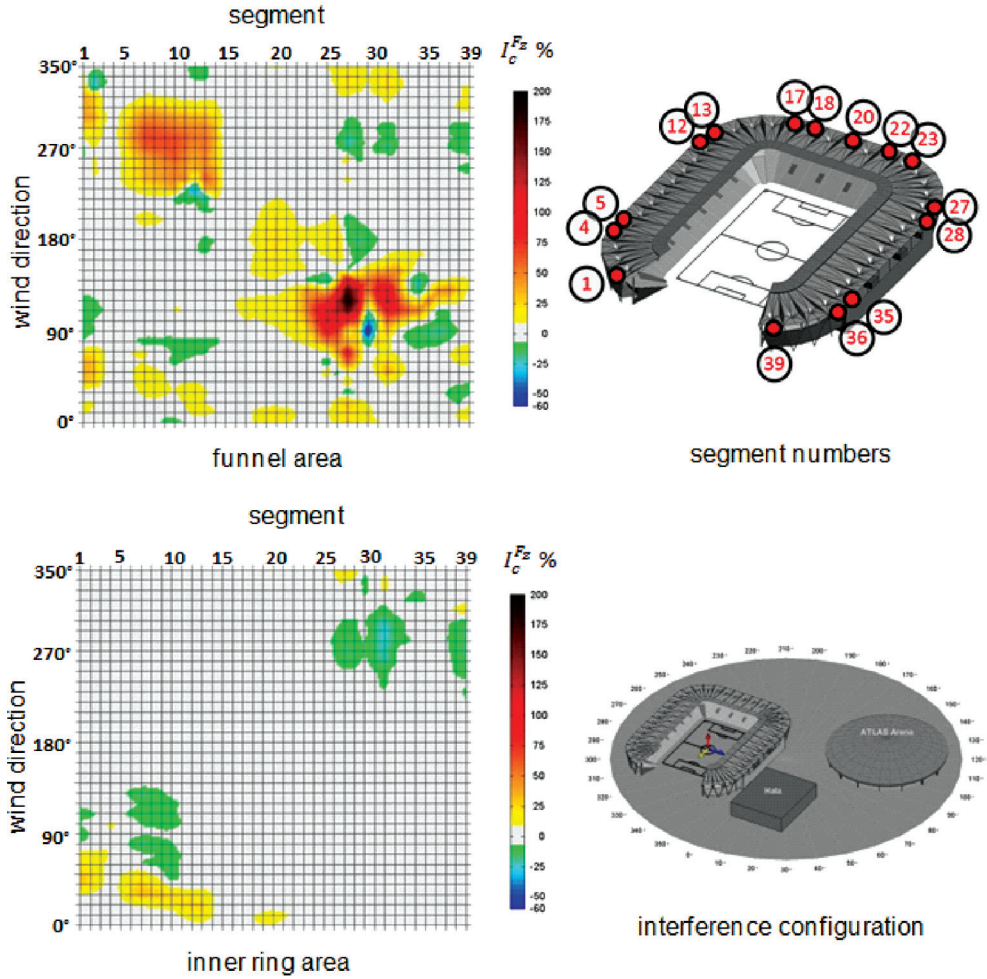


Fig. 13. Distributions of I_c^F coefficient in the interference configuration

4. Conclusions

The results of the measurements which were carried out in the wind tunnel allow for the formulation of the following conclusions:

- The open geometry of the stadium roof caused unfavourable aerodynamic effects. A significant uplift wind load for the part of the roof located on the opposite side to the open region of the stadium was observed for wind directions described by the near angles equal to 0° .
- The funnel shape of the stadium roof membrane caused significant variation of wind pressure distribution on the analysed surfaces. The leeward membrane area behind the roof funnel was exposed to a positive net wind pressure which pressed this roof region down. This

was a result of the appearance of the funnel wake at the bottom of the stadium membrane. The windward region was lifted where the significant negative net wind pressure occurred.

- The wind tunnel tests showed the significant influence of aerodynamic interference as a result of the proximity of the training hall and the sports-event hall with the stadium structure but the effect was limited to the confined stadium roof area situated near the neighbouring structure. The effect of aerodynamic interference consisted largely of pressing the roof membrane down in part of the funnel area, whereas for the inner ring area, this kind of wind load change is not observed.
- The measurements of the wind velocity absolute value, accomplished over the playing field of the stadium, showed an existence of an air flow ram effect. The nature of the effect, similar to the Venturi tube phenomenon, significantly increased the enormous lifting wind load on the part of the stadium roof located on the opposite side to the open region.

References

- [1] Józwiak R., Kasprzyk J., Żurański J.A., *Wind tunnel tests of a cable supported roof of a stadium*, Proc. of 10th ICWE, Copenhagen 1999, 1511–1517.
- [2] Bosak G., *Wind tunnel tests of aerodynamic interference of double-shell tanks*, Czasopismo Techniczne, 3B/2012, 3–19.
- [3] Borri C., Biagini P., *Structural response of large stadium roofs due to dynamic wind actions*, Stahlbau 74, Heft 3, 2005, 197–206.
- [4] Zhu L.D., Chen W., Shi Z.C., Zhang F., *Wind pressure distribution on a stadium roof by wind tunnel model test*, Proc. of 10th ICWE, Copenhagen 1999, 1583–1590.